Elektrotech. Inftech. (2023) 140:645–661
https://doi.org/10.1007/s00502-023-01180-y

e+i elektrotechnik und informationstechnik

Electromagnetic interference and the effect of low-voltage protective measures at electric vehicle charging stations

Martin Fürnschuß · Daniel Herbst · Peter Reichel · Daniel Stahleder · Christian Auer · Ernst Schmautzer · Robert Schürhuber

Received: 16 August 2023 / Accepted: 3 October 2023 / Published online: 15 November 2023

Abstract The nominal power of electric vehicle charging stations or charging parks is constantly increasing. Most of the users are ordinary persons and handle such equipment with a rated power of several 100 kW. Until now, equipment with such power ratings was only common in electrical operating facilities such as industrial plants where the users are at least instructed and protective measures are specified. If ordinary persons handle equipment with such power ratings in the field, the question arises as to whether the conventional safety goals are met in the event of an electrical fault. The consideration is: If the power increases so much, it can be assumed that the short-circuit power and thus the fault current increase and so does the risk of a dangerous electric shock. In this contribution, calculations of line-to-earth short-circuits on the low-voltage AC side of the three-phase system and their effects in typical configurations of charging stations are carried out. Considering the electromagnetic interference, the calculations provide the fault current and its distribution to determine the electrical potentials during the fault. From this, the (partial) fault voltages and active fault voltages are calculated. Based on the active fault voltage, the expected body impedance and consequently, the body current can be determined. With the body current and the break time of the protection device the risk of electric shock using international standards as guidelines is evaluated. As a result, recommendations for the planning, installation and safe operation of charging stations are given. It turns out that considering certain aspects like the conductor cross-sections or the electromagnetic interference, the risk of electric shock can be reduced to a conventional level. Periodic testing of the electrical system is necessary for safe and reliable operation. For example, follow-on faults due to unintended, improper use by ordinary persons can be prevented. Also, regular inspection of the electrical system is necessary for safe and reliable operation to prevent hazards due to aging or wear. However, it seems challenging to define an installation guideline that applies to all configurations as the boundary conditions vary depending on the type of system, installations in the area of interference and environmental influences.

Keywords Electric vehicle charging station · Protective measures · Body impedance · Body current · Earthing · Equipotential bonding · Electromagnetic interference

M. Fürnschuß, D. Herbst, P. Reichel, C. Auer, E. Schmautzer and R. Schürhuber are OVE members.

M. Fürnschuß (✉) · D. Herbst · R. Schürhuber
Institute of Electrical Power Systems, Graz University of Technology, Inffeldgasse 18, 8010 Graz, Austria
martin.fuernschuss@tugraz.at

P. Reichel
OVE—Österreichischer Verband für Elektrotechnik, Vienna, Austria

D. Stahleder
AIT—Austrian Institute of Technology, Vienna, Austria

C. Auer
KS Engineers—Kristl, Seibt & Co GmbH, Graz, Austria

E. Schmautzer
ESC—Engineering Services & Consulting GmbH, Graz, Austria

Elektromagnetische Beeinflussung und die Wirkung von Niederspannungsschutzmaßnahmen bei Ladestationen für Elektrofahrzeuge

Zusammenfassung Die Anschlussleistung von Ladestationen bzw. Ladeparks für Elektrofahrzeuge erhöhen sich ständig. So hantieren die Benutzer,

welche meist elektrotechnische Laien sind, mit Betriebsmitteln, welche Nennleistungen von mehreren 100 kW haben können. Üblich waren Betriebsmittel mit solchen Nennleistungen bis vor Kurzem nur in elektrischen Betriebsstätten wie z. B. Industriebetrieben, wo die Benutzer zumindest unterwiesen sind und spezielle Anforderungen an die Schutzmaßnahmen und -vorkehrungen gestellt werden. Hantieren Laien im Feld mit Betriebsmitteln in dieser Leistungsklasse, stellt sich die Frage, ob die vereinbarten Schutzziele bei einem elektrischen (Isolations-)Fehler erreicht werden. Die Überlegung dahinter ist folgende: Wenn die Anschlussleistung steigt, ist davon auszugehen, dass ebenso der Fehlerstrom steigt und sich dadurch das Risiko eines elektrischen Schlages erhöht. In diesem Beitrag werden Berechnungen von Erdkurzschlüssen auf Seite der Niederspannungs-Drehstromversorgung und deren Auswirkungen bei typischen Anordnungen von Ladestationen durchgeführt. Die Berechnungen liefern unter Berücksichtigung der elektromagnetischen Beeinflussung den Fehlerstrom und dessen Aufteilung, um die elektrischen Potenziale zu bestimmen. Daraus werden die im Fehlerfall auftretenden (Teil-)Fehlerspannungen und Wirkfehlerspannungen berechnet. Anhand der Wirkfehlerspannung lässt sich die zu erwartende Körperimpedanz und infolgedessen der Strom, der durch eine Person bei Berührung leitfähiger Teile fließt, bestimmen. Mit dem sogenannten Körperstrom und der Ausschaltzeit der Schutzeinrichtung wird die Gefährdung eines elektrischen Schlages auf Basis internationaler Normen evaluiert. Resultierend werden Empfehlungen für die Errichtung und den sicheren Betrieb von Ladestationen gegeben. Es zeigt sich, dass unter Berücksichtigung wichtiger Aspekte, wie z. B. dem Leitungsquerschnitt oder der elektromagnetischen Beeinflussung, die Reduktion des Risikos eines elektrischen Schlages auf ein gesellschaftlich vertretbares Niveau möglich ist. Eine regelmäßige Überprüfung der elektrischen Anlage ist für den sicheren und zuverlässigen Betrieb erforderlich. Ebenso ist eine regelmäßige Inspektion der elektrischen Anlage für den sicheren und zuverlässigen Betrieb notwendig, um Gefährdungen wie durch Alterung oder Verschleiß zu vermeiden. So können z. B. Folgefehler aufgrund von unwissentlicher, unsachgemäßer Benutzung durch Laien hintangehalten werden. Eine einheitliche Festlegung von Errichtungsvorschriften, welche sämtliche Konfigurationsmöglichkeiten einschließt, stellt eine große Herausforderung dar, da die Randbedingungen je nach Art der Anlage, Installationen im Beeinflussungsbereich und Umgebungseinflüssen variieren.

Schlüsselwörter Ladestation für Elektrofahrzeuge · Schutzmaßnahmen und -vorkehrungen · Körperimpedanz · Körperstrom · Erdung · Potenzialausgleich · Elektromagnetische Beeinflussung

1 Introduction

A couple of years ago, battery electric vehicles for individual mobility were niche products that hardly attracted any attention in the field of electrical engineering. They were usually charged via standard household sockets (e.g. in Austria IEC type F). The massive technological progress in the automotive industry has resulted in increased charging power in the last couple of years. This has allowed a significant reduction of the charging times. In the early years a maximum of 3.68 kW was usually available to the user via the protective contact socket. Today, common d.c. electrical vehicle charging stations have a rated power of 300 kW and more. They are publicly accessible and operated by ordinary persons. The power supply is mostly a three-phase low-voltage grid. Recently electrical equipment with such power ratings was primarily found in installations with restricted access such as industrial installations. In those, it can be assumed that only skilled or instructed persons have access to operate such powerful equipment.

If ordinary persons operate equipment in this power range in the open field – from warehouses to service stations – during all forms of weather, the question arises if the common protective measures are still sufficient or how they should be applied that the conventional protective goals are met; not only for normal use, but also for the expected use, which also includes misuse.

From the electrotechnical perspective, a serious fault in a charging station is a line-to-earth short-circuit, where a person touches a voltage directly or indirectly of accessible parts and suffers an electric shock. To prevent this, fault currents must be conducted in a controlled way and the touchable voltages have be limited to conventional values. For this purpose, line-to-earth short-circuits at charging stations connected to a TN-S system are calculated. The results of the short-circuit currents, conductor potentials, earth-surface voltages and the (partial) fault voltages are analysed under consideration of ohmic/inductive interference.

2 Methodology

2.1 Modell

A custom-made model, which is schematically shown in Fig. 1, is used as the investigation area. The model illustrates an usual electrical installation with a transforming station as power supply, two free-standing charging stations and a carport with six charging stations. Furthermore, the transforming station supplies two lighting masts. The entire facility is enclosed on two sides by a metal fence.

The enclosure of the transforming station is made of metal and galvanically connected to its earthing system, consisting of a ring earthing electrode and

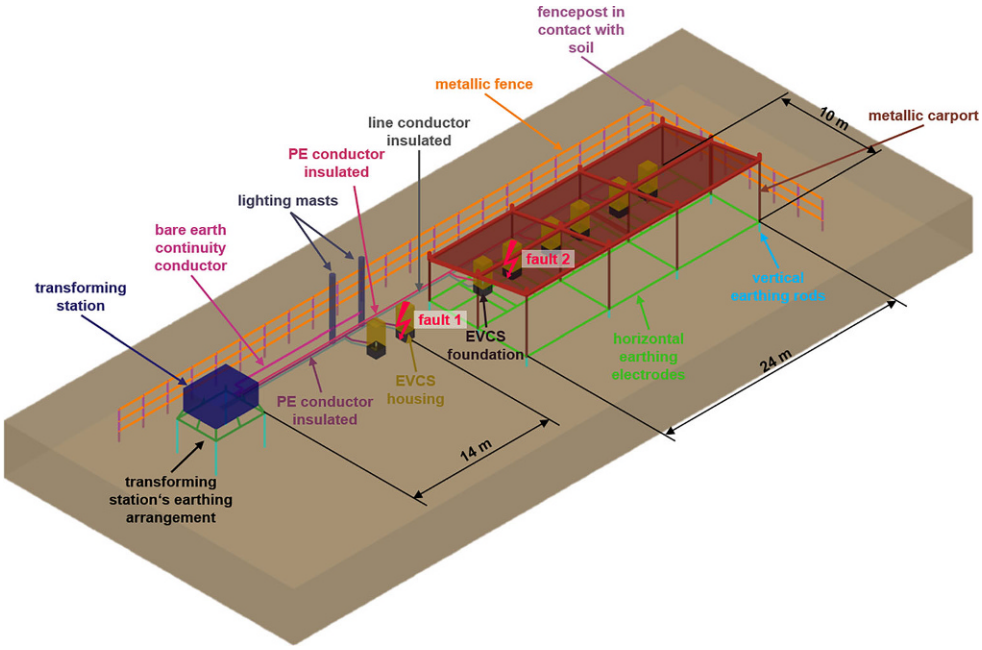

Fig. 1 Schematic illustration of the model

four earthing rods. The charging stations are class I equipment. For supply, line conductors with 95 mm² cross section are used. Each charging station has an earthed, electrically conductive foundation of reinforced concrete which is galvanically connected to the insulated protective earthing conductor (50 mm²) and the enclosure. The protective earthing conductor is also connected to the earthing arrangement of the transforming station. The carport is steel built and galvanically connected to the associated local earthing arrangement, which also serves as an equipotential bonding system. Via another low-voltage feeder, the transforming station supplies two metal lighting masts, whose foundations are earth-sensitive and electrically conductive. The lighting masts are connected to the transforming station's earthing arrangement via a bare earth continuity conductor. The fence foundations are in direct contact with earth and are considered as electrical conductors. The fencing is not galvanically connected to other parts of the installation.

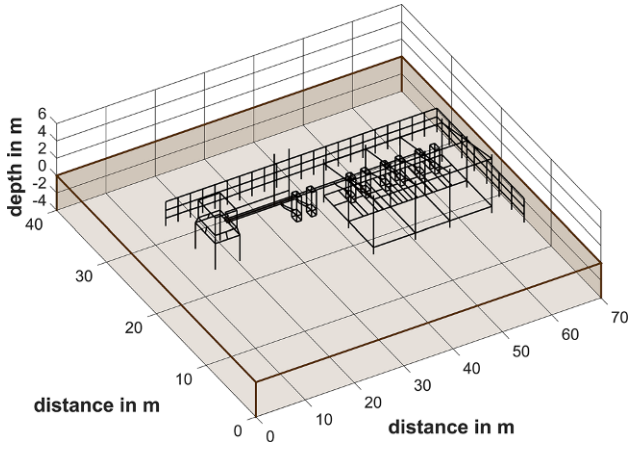

Fig. 2 Electrical conductor model

With these assumptions, an electrical conductor model as shown in Fig. 2 is created with a CAD-programme for the schematic model represented in Fig. 1.

The black solid lines in Fig. 2 and in the figures with the calculation results represent electrical conductors like phase conductors, protective earthing conductors, earthing electrodes, foundations, enclosures or metal constructions. The earth is represented with the brown coloured cuboid.

2.2 Definitions using a principle example

The terminology of potentials, voltages and currents used in this contribution is defined according to the principle example in Fig. 3, where two current-carrying vertical rods of different lengths are shown exemplarily.

As shown in Fig. 3, if a fault occurs from a line conductor to an earthed, electrically conductive part like the rods, the fault current I_F is conducted via the rods to the earth. Its magnitude depends on the line-earth voltage U_0 and the impedances to earth of the rods. Because of their electromagnetic interference, their impedances to earth are in turn depending on their geometric dimensions and arrangement. This results most often in an asymmetric distribution of I_F. Therefore, I_{E1} and I_{E2} in Fig. 3 can have different amperages. Both flow via the soil back to the earthed power supply. Due to the electrical resistance of the soil, the earth currents cause an increase in the earth-surface voltage φ. Strictly analytically, the earth-surface voltage is zero at infinity. That's the reason why for all considerations of potentials and voltages the

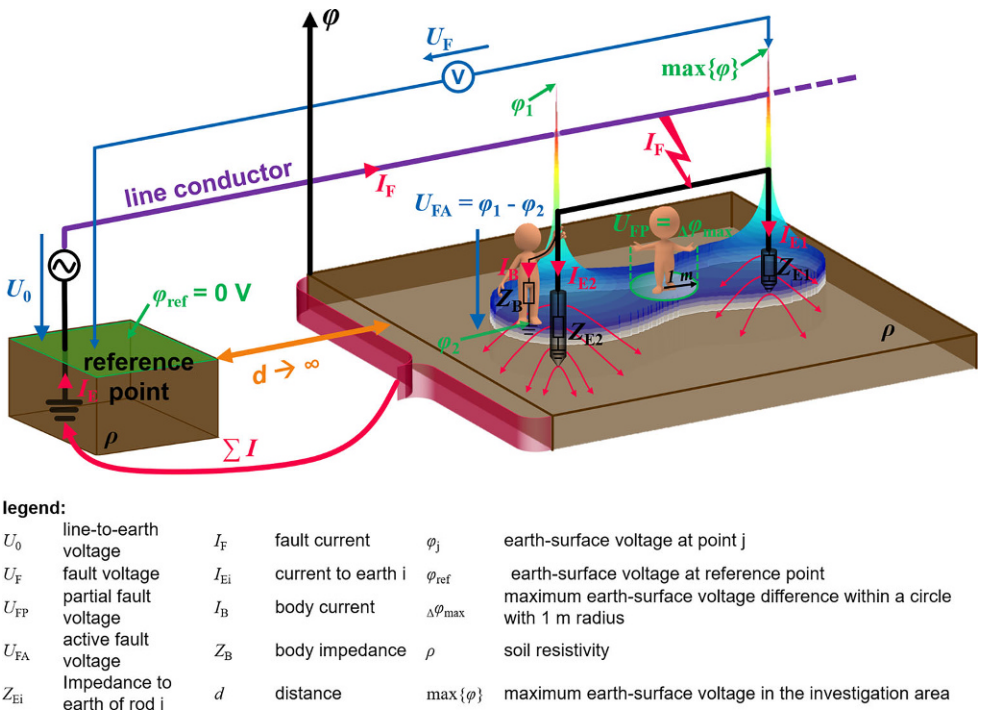

Fig. 3 Principle example for definition of voltages and currents

reference point is at infinity. The fault voltage U_F is defined as the maximum potential difference from the investigation area to the reference point according to Eq. 1. By the stated definition, $\varphi_{ref} := 0$, and therefore U_F is equal to $\max\{\varphi\}$.

$$U_F := \max\{\varphi\} \tag{1}$$

The partial fault voltages U_{FP} are calculated for each point in a 0.1 m grid of the earth-surface voltage φ in the sense of a worst-case consideration as maximum difference within a 1 m radius. All partial fault voltages are prospective ones – without considering additional impedances such as clothing, footwear, gloves or high resistivity surface materials e.g. tarmac.

Touches a person simultaneously two points with different electrical potential, a voltage drops across the body, the so-called active fault voltage U_{FA}. The active fault voltage is calculated by taking the difference between the potentials of the points/parts simultaneously touched. Accessible points/parts are for example, metallic overground installation components or the earth's surface. In case both points of touch are on the earth's surface, it is also called step voltage. Because of the active fault voltage, a current flows over the human body, the body current I_B. The body current is limited by the body impedance Z_B, which is dependent, among other things, on the magnitude of the active fault voltage. Values for the voltage- and frequency-dependent body impedance are published in international standards [2–7] and relevant literature [8–10].

2.3 Calculations

The line-to-earth short-circuit via the enclosure is investigated, and a distinction is made between two fault locations:

1. Fault 1: line-to-earth short-circuit at free-standing charging station
2. Fault 2: line-to-earth short-circuit in charging park

The two fault locations are shown in Fig. 1 (fault 1 and fault 2). For the he calculations a homogeneous soil with a specific earth resistance of $\rho = 100\ \Omega$m is assumed. The line-to-earth voltage U_0 is 230 V at a nominal frequency of 50 Hz. The transformer is modelled as an ideal voltage source. The fault current I_F is location-dependent due to the different conductor impedances and impedances to earth.

Calculations are carried out using the Peec technique [1], considering the ohmic-inductive interference, and the evaluation is performed using MATLAB. Electrical potentials and voltage drops are calculated in power supply lines and earth electrodes. All potentials, voltages and currents are root-mean-square values.

Referring to Eq. 2, the body current I_B is calculated using Ohm's law.

$$I_B = \frac{U_{FA}}{Z_B} \tag{2}$$

The fault current I_F is the basis for all further calculations. With its distribution, the currents to earth, the conductor potentials, the earth-surface voltage, the fault voltage, the partial fault voltages as well as

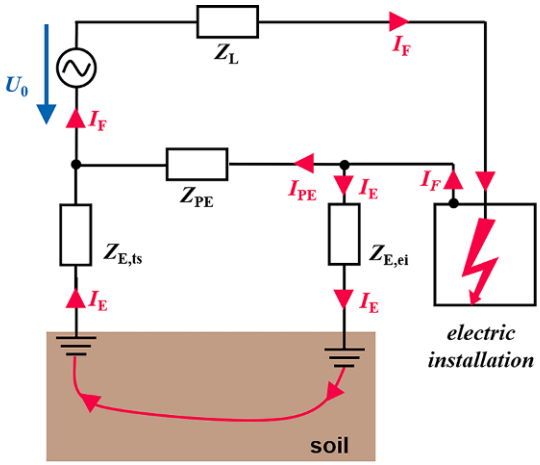

legend:

Z_L	line impedance	I_F	fault current
Z_{PE}	impedance of protective earth conductor	I_{PE}	current protective earthing conductor
$Z_{E,ts}$	impedance to earth transforming station	I_{PE1}	current protective earthing conductor 1
$Z_{E,ei}$	impedance to earth electric installation	U_0	line-to-earth voltage

Fig. 4 Simplified line diagram of an electric fault

the active fault voltages resulting body currents can be calculated.

The fault current's amperage is calculated by dividing the known line-to-earth voltage U_0 (230 V) by the fault impedance Z_F according to Eq. 3.

$$I_F = \frac{U_0}{Z_F} \tag{3}$$

The fault impedance depends on the fault location and is calculated of the active conductors and the impedances to earth, which are in ohmic and inductive interference.

As an example, the simplified line diagram of an earth fault is shown in Fig. 4. This simple calculation example neglects the electromagnetic interference between the conductors and earth.

Using Eq. 3, the fault current is calculated by determing the fault impedance Z_F according to Eq. 4:

$$Z_F = Z_L + \frac{Z_{PE} \cdot (Z_{E,ei} + Z_{E,ts})}{Z_{PE} + Z_{E,ei} + Z_{E,ts}} \tag{4}$$

3 Fault 1 – free-standing charging station

3.1 Current distributions

If there is short circuit from a line conductor to the enclosure at a free-standing charging station, the fault current is distributed from the enclosure to the protective earthing conductor and the foundation of the

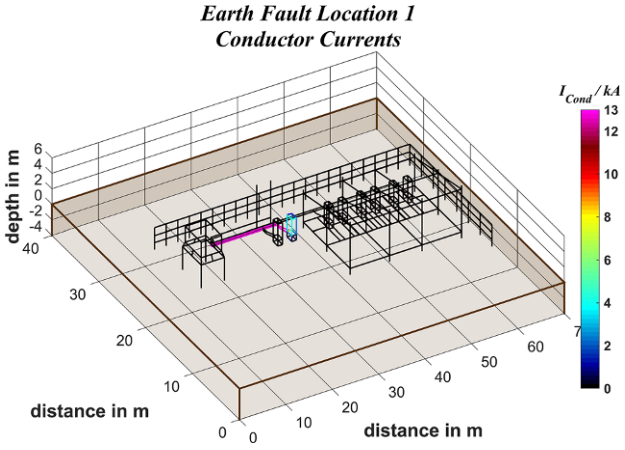

Fig. 5 Fault 1 – conductor currents, scaling full range (0 – 13 kA)

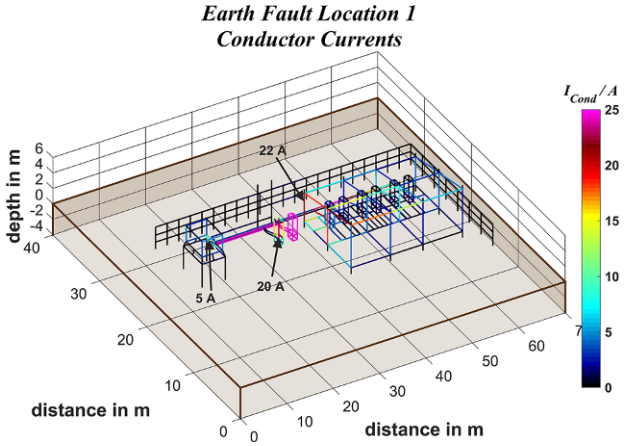

Fig. 6 Fault 1 – conductor currents, scaling range 0 – 25 A

charging station. A part of the currents in the foundation dissipate to earth. All partial fault currents flow back to the transformer neutral point. Figures 5 and 6 show the current distributions in the conductors at different scaling.

Figure 5 shows that a major part of the fault current of approximately 13 kA is conducted through the protective earthing conductor straight to the transformer neutral point. As seen in Fig. 6a small part returns to the neutral point via the galvanic bonded electrical installations via their connected protective earthing conductor as well as via the earth. The amperages reach the following maximum values (rounded) in the nearby electrical conductors:

- carport: 22 A
- nearby charging station: 20 A
- enclosure transforming station: 5 A

Currents up to 1.5 A flow in the fence in the close to the fault location and 1.9 A in the earth continuity conductor (ECC) connected to the lighting masts.

For the complete identification of the current distribution further calculations have to be done because: A part of the conductors are in direct contact with

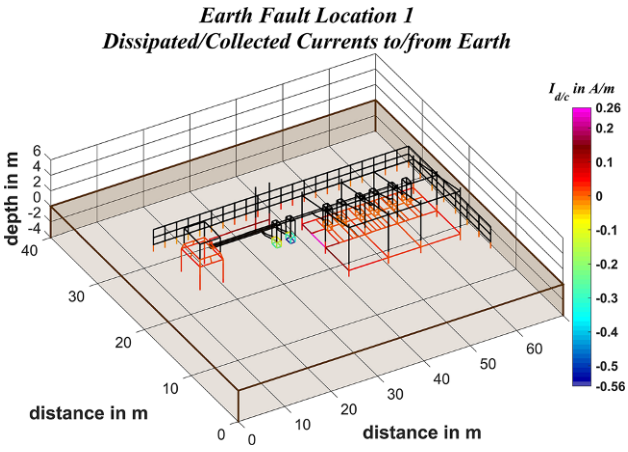

Fig. 7 Fault 1 – dissipated currents I_d to earth (negative) and collected currents I_c from earth (positive)

earth. The earth-sensitive conductors can dissipate electrical currents to the soil, but also collect earth currents. The results of these currents can be seen in Fig. 7. The sign of the currents in Fig. 7 indicate the direction of current flow: A negative sign indicates a current to earth, a positive a collected current from earth.

The foundations of the two free-standing charging stations dissipate currents to the earth. At the faulty charging station, the currents per unit length are maximum. The earth-sensitive conductors of the roofed charging park collect earth currents which are highest in the vicinity of the faulty charging station. This also explains the conductor currents in the earthing and equipotential bonding system of the roofed charging park: The currents flow from the soil into the earthing and equipotential bonding system of the charging park due to the ohmic/inductive interference. From there, they are distributed to all galvanically connected conductive elements and are returned to the transformer neutral point via the protective earthing conductors of the charging stations.

The same principle applies to the lighting masts and the connected earth continuity conductor. The earth continuity conductor carries the currents collected by the foundations to the transformer neutral point and collects earth currents on its entire length. Consequently, the current density increases per unit length to the transforming station.

In this example the earthing arrangement of the transforming station acts only as a sink of earth currents. For the vertical rods, the current collection per unit length increases with depth, which confirms the findings of [11]. The fence foundations collect currents from the earth in the vicinity of the fault location and dissipates them in the direction of the transforming station and the roofed charging park. The maximum dissipated currents per metre are in the vicinity of the transforming station; its earthing arrangement acts via the soil as a sink for the earth currents.

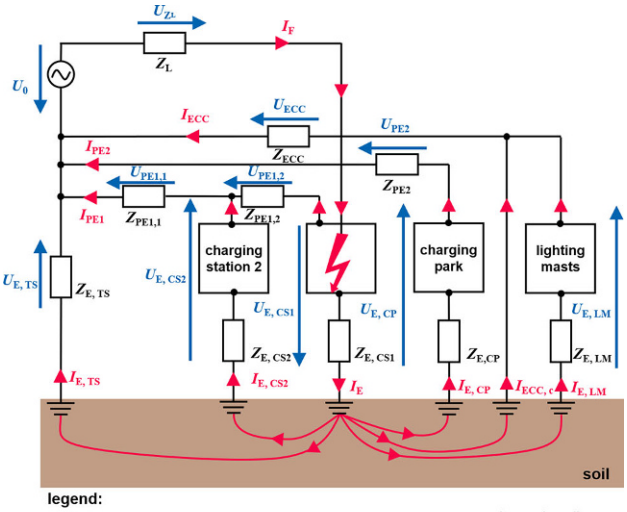

legend:

Z_L	line impedance	I_F	fault current	U_{ZL}	voltage drop line impedance
Z_{ECC}	impedance of earth continuity conductor	$I_{ECC,c}$	collected current from earth continuity conductor	U_{ECC}	voltage drop earth continuity conductor
		I_{ECC}	total current earth continuity conductor		
Z_{PE2}	impedance of protective earthing conductor 2	I_{PE2}	current protective earthing conductor 2	U_{PE2}	voltage drop protective earthing conductor 2
$Z_{PE1,1}$ $Z_{PE1,2}$	impedances of protective earthing conductor 1	I_{PE1}	current protective earthing conductor 1	$U_{PE1,1}$ $U_{PE1,2}$	voltage drops along protective earthing conductor 1
$Z_{E,TS}$	impedance to earth of transforming station	$I_{E,TS}$	collected current from earth transforming station	$U_{E,TS}$	partial fault voltage transforming station
$Z_{E,CS2}$	impedance to earth of charging station 2	$I_{E,CS2}$	collected current from earth charging station 2	$U_{E,CS2}$	collected current from earth charging station 2
$Z_{E,CS1}$	impedance to earth of charging station 1	I_E	current to earth	$U_{E,CS1}$	partial fault voltage charging station 1
$Z_{E,CP}$	impedance to earth of charging park	$I_{E,CP}$	collected current from earth charging park	$U_{E,CP}$	partial fault voltage charging park
$Z_{E,LM}$	impedance to earth of lighting masts	$I_{E,LM}$	collected current from earth lighting masts	$U_{E,LM}$	partial fault voltage lighting masts

Fig. 8 Fault 1 – equivalent circuit diagram with related impedances, currents and voltages

3.2 Conductor potentials

Based on the calculation results of the current distributions, the equivalent single-line circuit diagram according to Fig. 8 is drawn, where the current orientations are shown.

The currents cause voltage drops along the impedances, which result from potential differences between different locations.

Figures 9 and 10 show the potentials along the electrical conductors during the line-to-earth short-circuit with different scaling.

The accessible conductive parts are separated into areas with different potential levels:

- faulty charging station CS2
- free-standing charging station CS1
- transforming station
- lighting masts
- roofed charging park
- fence

The voltage drop along the line conductor from the transforming station to the fault location is 97.3 V, re-

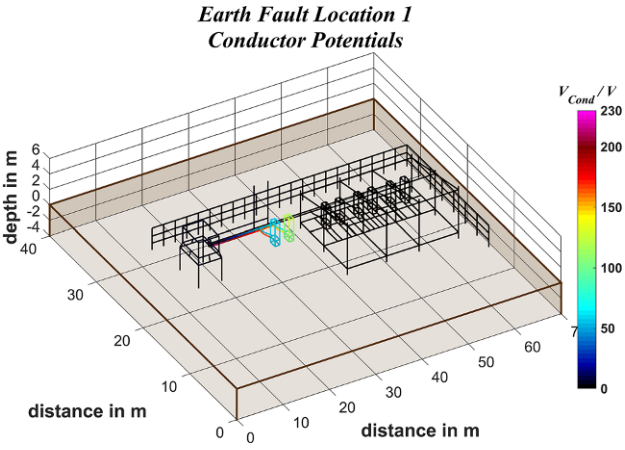

Fig. 9 Fault 1 – conductor potentials V_{Cond}, scaling full range

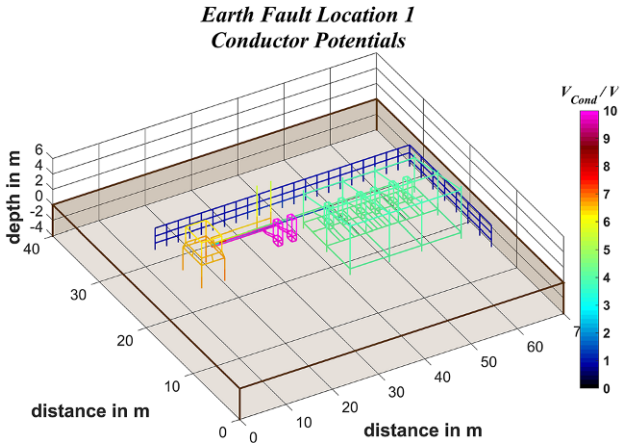

Fig. 10 Fault 1 – conductor potentials V_{Cond}, scaling range 0–10 V

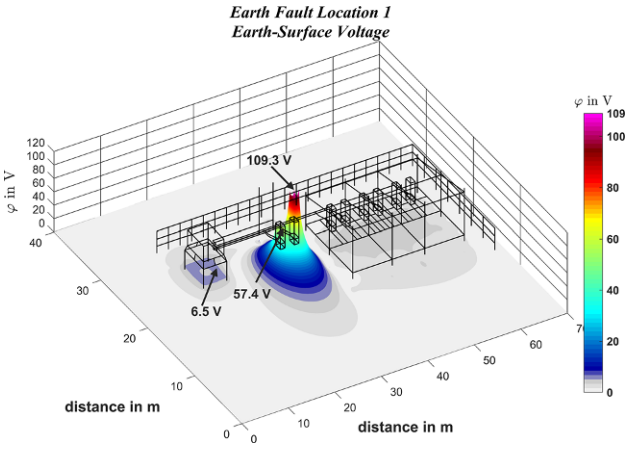

Fig. 11 Fault 1 – earth-surface voltage φ 3D view

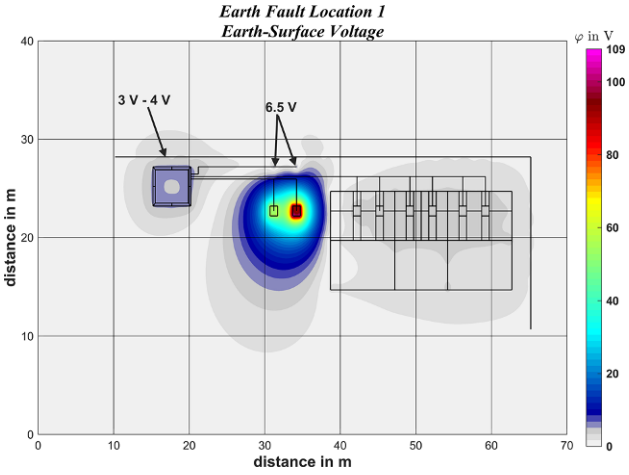

Fig. 12 Fault 1 – earth-surface voltage φ 2D view

sulting in a potential of 132.7 V at the enclosure of the charging station. These 132.7 V drop via the protective earthing conductor to the transformer neutral point. The close free-standing charging station CS1 is connected to the same protective earthing conductor and has a potential of 58.5 V. The potential of the transforming station's enclosure is maximum 6.6 V. The potential maximum of the conductors of the earthing and equipotential bonding system of the charging park above the surface is at the nearest pillar to the faulty charging station and is 4.5 V. The maximum potential of the metal lighting masts is 6.4 V. At the elements of the fence that are accessible for touching, the conductor potential assumes a maximum of 1.4 V in the immediate vicinity of the faulty charging station.

3.3 Earth-surface voltage

The calculation results of the current distributions (Chap. 3.1) and the conductor potentials (Chap. 3.2) show that the highest amperages and conductor potentials occur in the primary fault path: line conductor – faulty charging station – protective earthing conductor – transformer neutral point. The fault can also cause interference with other parts of the installation, either through potential transfers or vagabonding currents. The calculation of the earth-surface voltage, shown in Figs. 11 and 12 confirms this.

The fault voltage of 109.3 V appears at the faulty charging station. At the second free-standing charging station, the earth-surface voltage maximum is 57.4 and 6.5 V at the transforming station and the lighting masts. An equipotential area with a peak value of 4.5 V is almost formed in the inside of the roofed charging park. The earth-surface voltage along the fence reaches its maximum in the area of the transforming station with a value between 3 and 4 V.

3.4 Partial fault voltages caused by the earth-surface voltage

The results of the partial fault voltages calculated from the earth-surface voltage are shown in Figs. 13 and 14.

The maximum partial fault voltage of 69.8 V occurs one metre from the faulty charging station CS2. The major part of the current to earth is dissipated via the

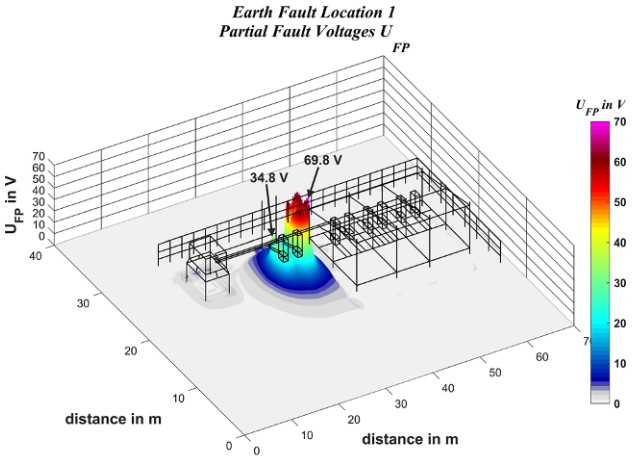

Fig. 13 Fault 1 – partial fault voltages U_{FP} 3D view

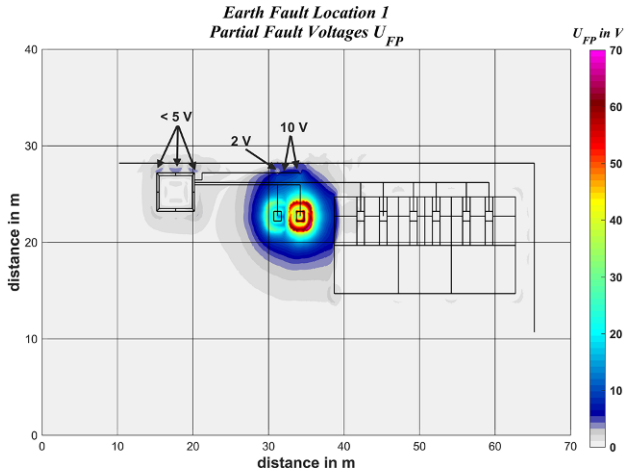

Fig. 14 Fault 1 – partial fault voltages U_{FP} 2D view

earth sensitive foundation (see Fig. 7) resulting in the highest partial fault voltages close to CS2.

At charging station CS1, the maximum partial fault voltage is 34.8 V. Between the two charging stations a region is formed where the partial fault voltages are smaller than at the outer edges. In this area, the effect of the electrical interference of the foundations becomes visible. Both can only dissipate lower amperages to the earth in these areas, which is why the partial fault voltages result in smaller values. For more detailed information on the interference of earth electrodes via the earth and the effects on the (partial) fault voltages, see publications [11, 12].

The lighting masts including the earth continuity conductor are located in the vicinity of interference of the faulty charging station, causing the partial fault voltages at the masts to be 10 V.

The earth currents that cannot flow back to the transformer neutral point via conductors like PE must return via the soil and the transforming station's earthing arrangement. The electromagnetic interference of their single earth electrodes results in partial fault voltages. These are below 5 V on all sides, and highest in the direction of the fence. As shown in Fig. 7, on this side the nearby fence foundations dissipate currents to the earth, which are mostly collected again by the nearest earth electrodes of the earthing arrangement.

3.5 Conclusions derived from example 1 considering the active fault voltages U_{FA}

The major part of the fault current of approximately 13 kA flows via the line conductor to the enclosure of the faulty charging station and from there via the protective earthing conductor back to the transforming station. This leads to voltage drops in conductors, potential gradients in earth and in consequence touchable potential differences. In a TN-S system with the protective measure automatic disconnection of supply, the break-time and therefore also the time in which voltages can be touched is limited. The principle is: With increasing amperage the fault time decreases.

This example assumes ideal connections – thus possible contact junction resistances are not taken into account. In order to return as much of the fault current as possible via the protective earthing conductor to the transformer neutral point, care must be taken to ensure that the conductor impedances and contact junction resistances are as low as possible. Low conductor impedances are achieved by using large cross-section and short conductor lengths. With increasing operating time, the contact resistances, e.g. to the charging station enclosure, can increase due to environmental influences like dirt or corrosion. A regular testing of the contact resistances is therefore necessary.

A relatively small part of the fault current flows back to the transformer neutral point via the earth and other installation components. Other risks can also occur in other, non-galvanically connected installations by their earthing and equipotential bonding systems due to the earth currents. These are manifested by vagabonding currents, which generate unwanted noise or partial fault voltages.

Providing the charging station is protection class I equipment and assuming that the equipotential bonding of the charging stations is functional, their enclosure is to be considered as an equipotential surface. Neglecting impedances which only occur during the fault, such as the arc impedance, the potential of the enclosure increases to the value of the nominal voltage to earth minus the voltage drop along the line conductor. If the enclosure is touched, the active fault voltage U_{FA} is relevant for the hazard evaluation of an electric shock. The active fault voltage is determined by the difference between the potentials of the touching points. For example, if a person next to the charging station touches the enclosure, the active fault voltage is calculated from the difference between the potential of the enclosure of the charging station and the earth-surface voltage. In this exam-

ple, the maximum active fault voltage when touching the enclosure is U_{FA} = 93.9 V. Without switching off the power supply, the limit of U_{FA} (50 V according to OVE E 8101:2019 + AC1:2020 [13]) is exceeded. One method decreasing the voltage would be the application of high resistive material (e.g. tarmac on gravel basement) on earth's surface in order not exceeding the conventional limit. However, this method is not considered to be an appropriate state of the art protective measure in main circuits in Austria due to the possibility of accessibility by ordinary persons (see OVE E 8101:2019 + AC1:2020- part 722 [13]). Another possibility to tap the maximum active fault voltage, even with existing location insulation, is to touch the faulty charging station and a metallic anti-ram protection at the same time. Is the anti-ram protection not integrated into the local equipotential bonding system, the maximum active fault voltage could be touched between both hands. The distance of two metres between the two free-standing charging stations allows both enclosures to be touched at the same time. In this hand to hand touch scenario, the active fault voltage is the potential difference between both enclosures and is 74.2 V.

4 Fault 2 – charging station carport

In this chapter, the calculation results for a line-to-earth short-circuit at a charging station in the carport are treated. Each charging station in the carport is galvanically connected on all four sides to the three-dimensional earthing and equipotential bonding system.

4.1 Current distributions

In the case of a line-to-earth short-circuit at a charging station, the fault current of 8.8 kA is distributed as illustrated in Figs. 15 and 16. The two figures of the conductor amperages differ in their scaling.

As in example 1 (Chap. 3, fault 1 at a free-standing charging station), the main fault current path is from the transforming station via the line conductor to the charging station enclosure back to the transformer neutral point via the protective earthing conductor. In example 1, where the majority of the fault current is conducted via the directly connected protective earthing conductor, in this case it is only approx. 65% (5.8 kA). Due to the integration into and the lower earthing impedance of the earthing and equipotential bonding system of the charging park, the fault current is distributed on the one hand over all galvanically connected conductors. On the other hand, a higher percentage of the fault current dissipates to earth.

The following maximum conductor amperages result in the individual installation parts:

- earthing and equipotential bonding system carport:
  - overground: 276 A
  - underground: 1 kA
  - enclosure adjacent charging stations 100 A
- free-standing charging stations:
  - enclosure: 1.1 A
  - PE-conductor: 4.3 A
- enclosure transforming station: 1.2 A
- earth continuity conductor lighting masts: 6.7 A
- fence: 1.8 A

To determine the current distribution, the currents dissipated or collected by the conductors in contact with the earth have been calculated and the results are shown in Fig. 17. The sign of the currents in Fig. 17 indicate the direction of current flow: A positive sign indicates a current to earth, a negative a collected current from earth.

The earth-sensitive part of the earthing and equipotential bonding system of the charging park only dissipates currents to the earth. As a pure current sink for the earth currents are acting:

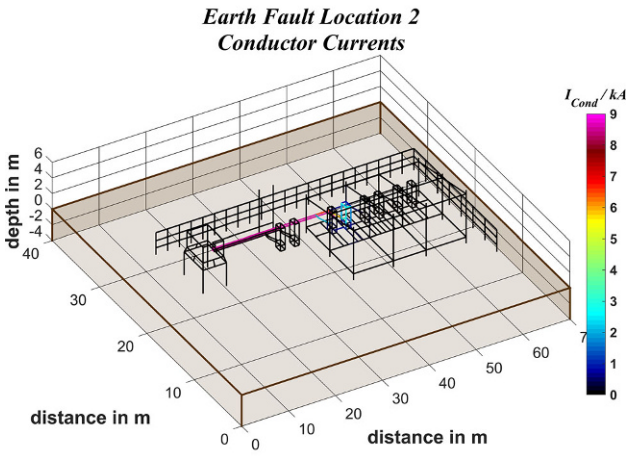

Fig. 15 Fault 2 – conductor currents I_{Cond}, scaling full range (0 – 9 kA)

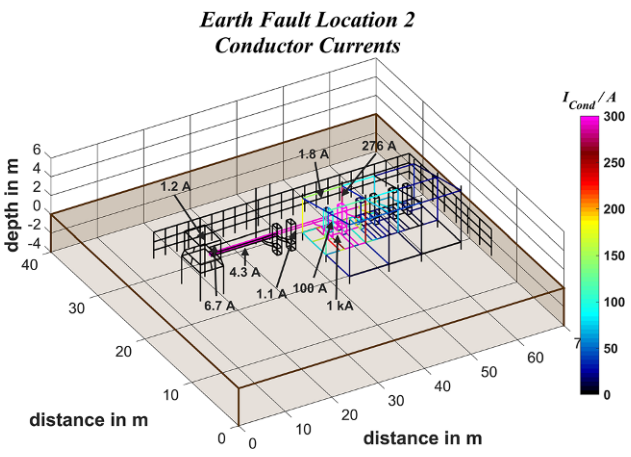

Fig. 16 Fault 2 – conductor currents I_{Cond}, scaling range 0 – 200 A

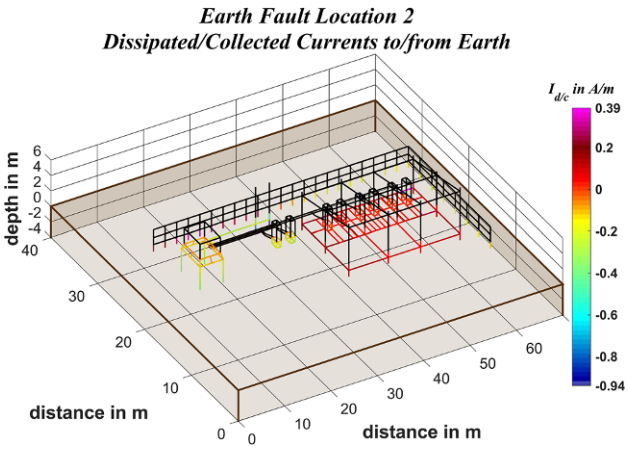

Fig. 17 Fault 2 – dissipated currents I_d to earth (positive) and collected currents I_c from earth (negative)

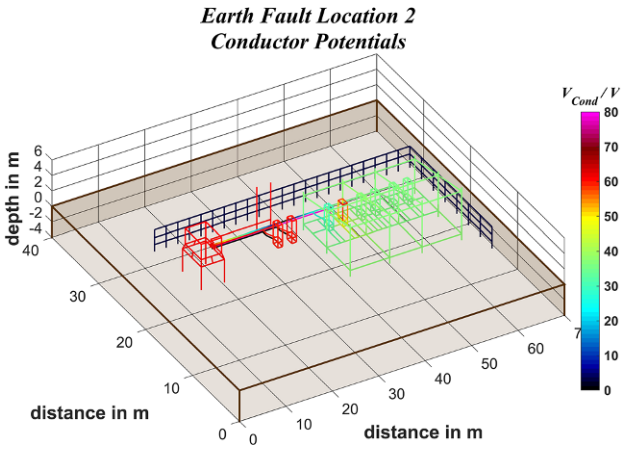

Fig. 19 Fault 2 – conductor potentials V_{Cond}, scaling range 0 – 80 V

- the foundations of the free-standing charging stations
- the earthing arrangement of the transforming station
- the foundations of the lighting masts and the galvanically connected earth continuity conductor.

In total, the three current sinks collect an earth current of 40 A.

The fence collects earth currents via its foundations in the area of the earthing and equipotential bonding system of the charging park and dissipates them in the vicinity of the transforming station. The dissipated currents per unit length increase in the direction of the transforming station's earthing arrangement.

4.2 Conductor potentials

Figures 18 and 19 show the distributions of the potentials on the electrical conductors during the short-circuit with different scaling.

The enclosure of the faulty charging station has a potential of 66.8 V. This results in a voltage drop from the transforming station via the line conductor to the fault location of 163.2 V. As the calculation results of the current distribution show, approx. one third of the fault current is not conducted to the transformer neutral point via the protective earthing conductor connected to the faulty charging station. This proportion vagabonds through the entire installation and causes varying potential rises. In the charging park itself, the conductor potentials, except at the fault location, are between 35 and 40 V. Compared to example 1, a higher proportion of the earth currents return to the transformer neutral point via the earthing arrangement of the transforming station, the foundations of the free-standing charging stations and earth continuity conductor of the lighting masts. This results in higher conductor potentials which are approx. 60 to 65 V. However, due to the galvanic connection of the transformer neutral point, the earthing arrangement of the transforming station and its enclosure, the free-standing charging stations and the lighting masts, have all almost the same potential. The elements of the fence have almost a constant potential between 3.8 and 4.2 V.

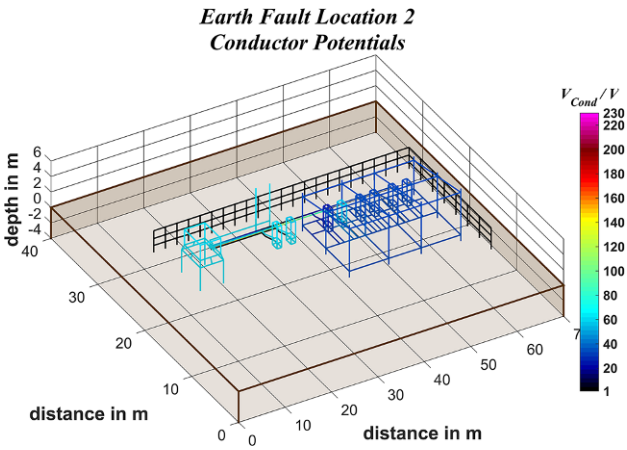

Fig. 18 Fault 2 – conductor potentials V_{Cond}, scaling full range (0 – 230 V)

4.3 Earth-surface voltage

The results of the earth-surface voltage, shown in Figs. 20 and 21, show a division into two areas: one is the charging park and the other the remaining electrical installation.

A 1 to 2 m wide corridor is formed on the left side of the charging park, where the earth-surface voltage is below 5 V (grey to light grey area in Fig. 21). The fault voltage is 61.7 V and, contrary to expectations, does not occur at the fault location but at the transforming station. At the faulty charging station, the earth-surface voltage is maximum 49.5 V. Inside the charging park, nearly an equipotential surface is formed 2 m away from the fault location, which decreases to 25 V towards the outside. The potential drop of the charging park at the edge of the construction is steeper than

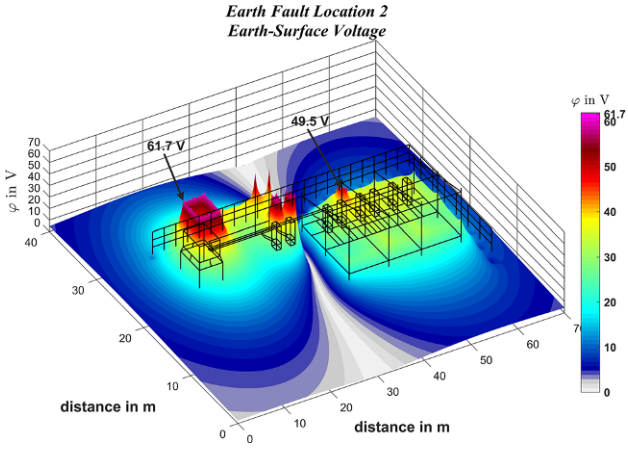

Fig. 20 Fault 2 – earth-surface voltage φ 3D view

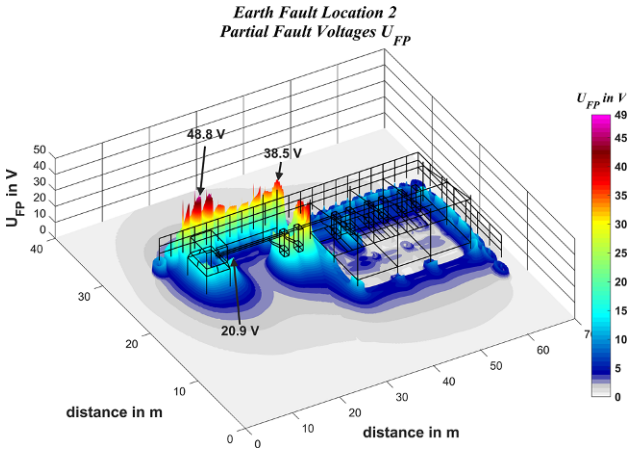

Fig. 22 Fault 2 – (partial) fault voltages U_{FP} 3D view

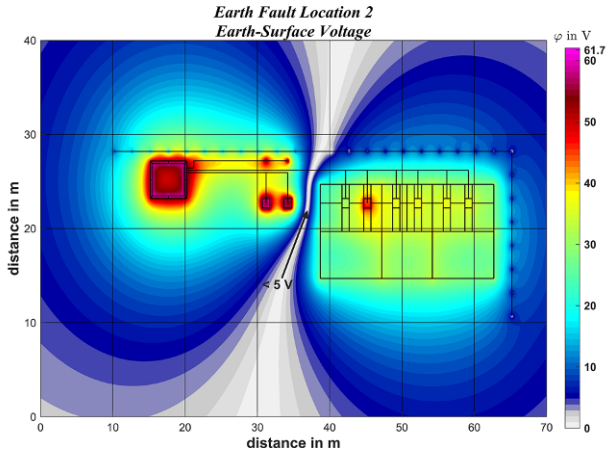

Fig. 21 Fault 2 – earth-surface voltage φ 2D view

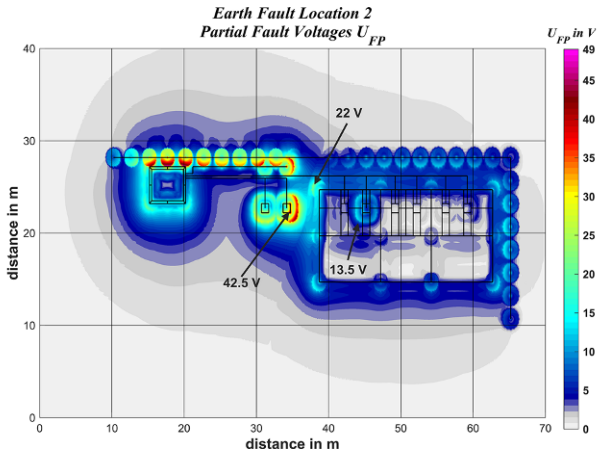

Fig. 23 Fault 2 – (partial) fault voltages U_{FP} 2D view

those of the transforming station, the free-standing charging stations and the lighting masts. At the fence foundations, the earth-surface voltage is significantly reduced compared to their immediate surroundings.

A comparison with the results for the earth-surface voltage of example 1 shows that the area of interference is significantly larger in the case of a line-to-earth short-circuit in the charging park. This is due to the higher earth currents and their distribution over a larger area.

4.4 Partial and active fault voltages

The partial fault voltages in Figs. 22 and 23 are calculated from the earth-surface voltage.

At the fault location the partial fault voltage reaches 13.6 V maximum. Since the calculations of the earth-surface voltage within the charging park, except for the fault location, provide almost an equipotential surface, the partial fault voltages are less than 5 V. The partial fault voltages that can be assigned to the charging park are highest for the metal pillars of the carport, especially in the outside area (up to 22 V). The pillars are integrated in the earthing and equipotential bonding system of the charging park and are considered vertical rods from an electrotechnical point of view. Due to the characteristics of vertical rods, the (partial) fault voltages are locally higher than at the horizontal earthing electrodes [11, 12, 14]. When touching the enclosure of the faulty charging station in the 1 m range, the maximum active fault voltage U_{FA} is 30.8 V. By touching the faulty charging station's enclosure to the charging station on the left (2 m distance) and assuming an electrical insulated surface, the active fault voltage is 31.5 V. The worst case when touching the steel structure is the outer rearmost upright at the edge towards the free-standing charging stations. Here, the maximum active fault voltage in the 1 m range is 22 V.

At the free-standing charging stations closest to the charging park, a maximum partial fault voltage of 42.5 V occurs. The maximum active fault voltage U_{FA} there is 47.8 V.

At the outer lighting masts, the maximum partial fault voltage U_{FP} is 38.5 V. Standing nearby this mast and touching it, the maximum active fault voltage U_{FA} is 37.2 V. An active fault voltage of 57.1 V results from simultaneously touching a lighting mast and the fence

system, which is spatially only one metre away (assumption: electrical insulation feet to earth).

At the transforming station itself, the maximum touchable partial fault voltage, calculated from the earth-surface voltage, is 20.9 V. The highest partial fault voltages are between the horizontal electrode of the transforming station's earthing arrangement and the fence system in the area of its foundations: Along the horizontal electrode the earth-surface voltage is between 50 and 60 V and at the fence pillars next to the transforming station between 4 and 8 V, resulting in a maximum partial fault voltage of 48.8 V at the middle fence pillar. There is a distance of 1.3 m between the transforming station's enclosure and the fence. If both hands touch the enclosure and the fence at the same time, an active fault voltage of 57.7 V is touched considering an electrically insulated earth-surface. When just touching the enclosure, the maximum active fault voltage within one metre is 25.9 V.

4.5 Conclusions derived from example 2 considering the active fault voltage U_{FA}

In the event of a line-to-earth short-circuit in the three-dimensional earthing and equipotential bonding system, two third of the fault current are conducted to the transformer neutral point via the protective earthing conductor of the faulty charging station. One third of the fault current vagabonds in the earthing and equipotential bonding system and a part is dissipated to earth. Except in the area of the faulty charging station, the conductor potentials in the earthing and equipotential bonding system are constant and an almost homogeneous earth-surface voltage is formed inside.

Compared to the calculation results in example 1, the partial fault voltages at the fault location are lower. Due to the longer conductor lengths, the short-circuit amperage is less than in example 1, but the current to earth is higher. The higher amperage of the current to earth results in a higher increase of the conductor potentials and the earth-surface voltage in the area of the transforming station's earthing arrangement, which are also transferred to the galvanically connected installations. The maximum active fault voltages are not at the fault location or inside the charging park, but outside at the following areas:

- enclosure transforming station to fence
- lighting mast to fence
- free-standing charging station

Example 2 shows that the three-dimensional earthing and equipotential bonding system of the roofed charging park in the purpose of the protective measure leads to a significant reduction of active fault voltages. If system parts are not integrated into the earthing system via earth electrodes, increased attention must be paid to possible transferred potentials. Furthermore, the higher earth currents can lead to interferences in other, galvanically isolated installations. Attention must also be paid to the distances between fencing systems and electrical installations. If these are in the hand or touch area, considerable active fault voltages can be detected. A corresponding integration into the earthing system or an electrical insulation of the fence can prevent this and reduce the active fault voltages. A sufficiently large protective earthing conductor cross-section must also be ensured. Due to the galvanic connection of the charging stations in the carport, the protective earthing conductors of the other charging stations also carries a significant proportion of the fault current back to the transforming station.

5 Expected body currents and conclusion

Calculation results of line-to-earth short-circuits at electric vehicle charging stations (EVCS) and their effects on active fault are shown. For this purpose, an exemplary model has been designed which is as close to reality as possible and which deals with individual, free-standing charging stations and a roofed charging park as well as additional lighting masts and a fence. The power is provided by a transforming station via a TN-S system with the protective measure automatic disconnection of supply. The state of art is reducing the break-time to conventional limits; e.g. max. 0.4 s in end circuits with nominal currents up to 32 A and 5 s in main power lines with nominal currents higher 32 A. This is common especially in end circuits where the risk of a hazardous electric shock is estimated to be higher than in distribution lines or lines in the grid. Protection against electric shock is thus more likely in end circuits than in main circuits. In the following, faults in main circuits are dealt with, taking into account the standard IEC 60479-1:2018 [2]. Two faults (low-voltage line-to-earth short circuits with an ideal electrical connection between a line conductor and the metallic enclosure) are defined:

- Fault 1: at a free-standing charging station
- Fault 2: at a charging station in the carport

5.1 Current distributions and fault voltages

In the case of fault 1, at the free-standing charging station with a simple earthing arrangement, the majority of the fault current returns to the transformer neutral point via the protective earthing conductor. The earth-surface voltages and the active fault voltages are limited to the area of the faulty charging station. The permissible limit of 50 V according to OVE E 8101:2019 + AC1:2020 [13] is exceeded by 44.3 V without switching off the power supply.

In the case of fault 2, in a charging park with an earthing and equipotential bonding system, the partial fault voltages at the fault location are smaller than in example 1. This reduction shows, that the meshed

three dimensional earthing and equipotential bonding system makes a significant contribution to protection against electric shock at the fault location. Within the charging park, the earth-surface voltage is almost homogeneous from a distance of 2 m of the fault location. Furthermore, the earthing and equipotential bonding system selectively conducts approximately one third of the fault current. However, the advantages at the location of the fault also imply disadvantages: The earth current amperages are higher than in example 1 due to the connection to the extensive three-dimensional meshed earthing and equipotential bonding system. Although the fault current amperage is lower by approx. 5 kA. An amperage of 3.8 kA return to the transformer neutral point via other parts of the installations that are in contact with the earth. The fence collects earth currents in the area of the charging park and dissipates them in the area of the transforming station—it acts like a parallel conductor to earth. As a consequence, the fence has a location depending electrical potential. The highest partial fault voltages in example 2 do not occur at the fault location, but at the installation parts located outside the charging park. The earthing arrangement of the transforming station has a much higher potential than in example 1, which is transferred to the lighting masts and the two free-standing charging stations.

5.2 Body currents

Electric vehicle charging stations with 100 kW have been selected for the calculations. In a power class of 22 kW and above, charging stations with d.c. vehicle connectors are common. In Austria, there is still no regulation, standard, guideline, etc. that requires the installation of a residual current device for d.c. charging stations. Increasing the connected load, for example to 300 kW per charging station, as is already common in practice, means that the conductor cross-section of the supply lines must also increase: both that of the line conductors and the protective earthing conductor. Therefore, the fault amperage will rise and an increase of the body current could be possible. A residual current monitoring unit (RCM) surely has advantages here, but the question arises to what power class the corresponding protective devices are available on the market. When applying the protective measure automatic disconnection of supply, the thermal fuse or circuit breaker must therefore switch off quickly. In the following, the expected body current is determined based on the previously calculated active fault voltages U_{FA}, using the standard IEC 60479-1:2018 as basic guideline [2]. The calculation results of the body impedances, as already mentioned in Chap. 2.2, do not consider additional impedances such as those caused by footwear or gloves in the sense of a worst-case perspective.

In example 1, hazards are possible due to touching conductive installation parts. When touching both enclosures of the free-standing charging station with one hand each and standing electrically insulated, a person can touch an active fault voltage of 74.3 V.

Now, according to IEC 60479-1:2018 [2] the body impedance can be considered to be $Z_T = 2000\,\Omega$ for a percentile rank of 50% of the population for touching a voltage of 75 V. This value is applicable for dry hands and a contact area of 10,000 mm^2. By application of Eq. 2 this results in a body current of 37 mA at 50 Hz for the calculated active fault voltage $U_{FA} = 74.3$ V.

For the current path, both hands to feet (enclosure to earth surface) the active fault voltage is 93.9 V. For a percentile rank of 50% of the population for touching a voltage of 100 V results in a body impedance of 690 Ω according to [2]. Using this value to calculate the body current and the calculation result for the active fault voltage of 93.9 V, the body current is 136 mA.

In example 2, the active fault voltages at the fault location are significantly lower due to the better earthing and equipotential bonding at the fault location and in the area of the charging park. Therefore, it can be assumed that the body currents, when touching at the fault location, are lower than in example 1. On the one hand they are lower due to the lower voltages and on the other hand due to the resulting higher body impedances.

With a current path from both hands to feet at the faulty charging station, an active fault voltage of $U_{FA} = 30.8$ V results in a body impedance of $Z_T = 1300\,\Omega$ for dry hands and a large area of contact according to [2] by using the value for the 50% percentile rank of the population of the hand to hand impedance for touching 25 V. The result of the body current by using the calculated active fault voltage is 23.7 mA.

For the current path hand to hand from the faulty charging station to the next charging station 2 m away (assumption electrical insulated earth surface), the active fault voltage is $U_{FA} = 36.3$ V. In this case, the body impedance is $Z_T = 3250\,\Omega$ for dry hands and a large area of contact according to [2] for the 50% percentile rank of the population for touching 25 V. The result of the body current is 11.1 mA using the calculated active fault voltage.

With a body current path hand to hand from the transformer enclosure to the fence system, a body impedance of $Z_T = 2500\,\Omega$ (value selected for 50 V and the 50% percentile rank for the population) results for an active fault voltage of 57.7 V and the same assumptions as in example 1. The resulting body current is 23.1 mA.

Touching a lighting mast by a body current path both hands to feet, the body impedance is 1000 Ω. With an active fault voltage of 37.7 V, the body current is calculated to be 37.7 mA.

Summarising, Table 1 shows the body currents for the two examples with the corresponding current paths.

The risk of ventricular fibrillation is dependent on the body current and the duration of current flow. For

Table 1 Calculation results of the body currents according to [2]

Fault 1: line-to-earth short-circuit at free-standing EVCS			
Touch location	Current path	Active fault voltage	Body current
–	–	V	mA
Faulty EVCS	Both hands to feet	93.9	136
Faulty EVCS to second free-standing EVCS	Hand to hand	74.3	37
Fault 2: line-to-earth short-circuit at EVCS in charging park			
Faulty EVCS	Both hands to feet	30.8	23.7
Faulty EVCS to next EVCS	Hand to hand	35.3	11.1
Lighting mast	Both hands to feet	37.7	37.7
Enclosure transforming station to fence	Hand to hand	57.7	23.1

Table 2 Converted body currents I_{ref} which represent the same danger of ventricular fibrillation as the corresponding current path left hand to feet

Fault 1: line-to-earth short-circuit at free-standing EVCS			
Touch location	Current path	I_h	I_{ref}
–	–	mA	mA
Faulty EVCS	Both hands to feet	136	136
Faulty EVCS to second free-EVCS	Hand to hand	37	14.8
Fault 2: line-to-earth short-circuit at EVCS in charging park			
Faulty EVCS	Both hands to feet	23.7	23.7
Faulty EVCS to next EVCS	Hand to hand	11.1	4.4
Lighting mast	Both hands to feet	37.7	37.7
Enclosure transforming station to fence	Hand to hand	23.1	9.2

the evaluation of the protection measure protection by automatic disconnection of supply concerning EN 60479-1, in the following Chap. 5.3 the connection between break-time and body current is made.

5.3 Protection by automatic disconnection of supply

It is possible that muscle contractions and ventricular fibrillation may already occur at the body currents according to Table 1 when the current is flowing in the vulnerable period [2]. Therefore, it is important to clear the fault as soon as possible. By selecting a 250 A thermal fuse as protective device, a break-time within 20 ms (one cycle) can be assumed. For this break-time and the calculated body currents the probability of ventricular fibrillation is negligible according to IEC 60479 standard series [2–7]. The conventional time/current zones according to [2] are used for the assessment. These are represented for a current path left hand to both feet as shown in Fig. 24 according to [2].

Since in this contribution the current path left hand to feet is not investigated, the calculated currents must be converted to values, which represent the same danger of ventricular fibrillation as for left hand to feet. For this, [2] provides values for the so-called heart-current factor F with which the calculated body currents from Table 1 can be converted. The relationship is given by Eq. 5

$$I_{ref} = I_h \cdot F \tag{5}$$

where I_{ref} is the body current for the path left hand to feet and I_h is the body current for the applicable current path.

The heart-current factors for the investigated current paths are according to Table 12 in [2]:

- $F = 1$: for both hands to feet
- $F = 0.4$: for hand to hand

Application of Eq. 5 results in the reference currents in Table 2:

Assuming a maximum break-time of 20 ms, all reference currents are in the zone AC-2 in Fig. 24 during fault 2 and except one, all currents exceed the threshold of the let-go current for the entire population of 5 mA according to [2]. Possible physiological effects could be perception and involuntary muscular contractions, but usually no harmful electrical physiological effects (see Table 11 in [2]). The value of $I_{ref} = 136$ mA for a fault at the free-standing charging station and the current path both hands to feet is close to the limit AC-2 to AC-3 in Fig. 24. It is important to note that all body currents apply for dry hands; if they are (salt-) wet (e.g. rain, salt wet in winter), the body currents increase significantly.

If the reference currents increase to amperages where the zone AC-3 is applicable, strong involuntary muscular contractions, difficulty in breathing, reversible disturbances of heart function and/or immobilization are possible (see Table 11 in [2]).

The maximum break-time of 5 s for TN-S systems for final circuits >32 A as required by OVE E 8101:2019 + AC1:2020 [13] seems far too high, when

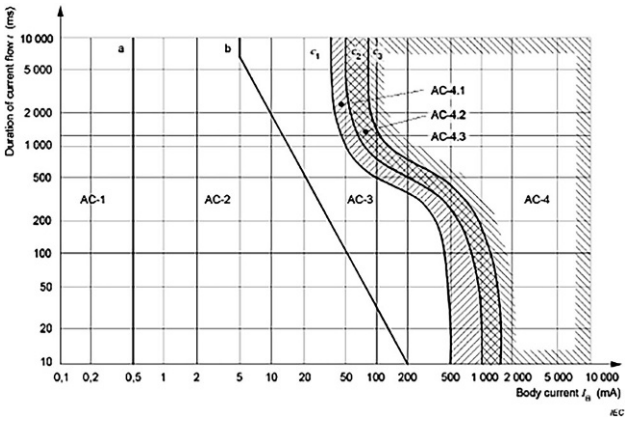

Fig. 24 Conventional time/current zones of effects of AC currents (15 to 100 Hz) on persons for a current path corresponding to left hand to feet (Fig. 20 in [2])

considering the possible body currents, if the risk of ventricular fibrillation is to be reduced to a conventional level in accordance with [2]. It is therefore important to switch off as fast as possible.

5.4 Suggestions for the construction and operation of charging stations

Regardless of the integration of the charging stations to a local earthing and equipotential bonding system, the current return path via the protective earthing conductor is of great importance. This current return path should be low impedant in order to conduct as much of the fault current as possible. Regular inspections of the entire fault loop, including contact resistances, clamping connections and cable lugs are recommended. Due to the possibility of potential transfers, avoidance measures must be considered before the installation is constructed. Special attention must be paid to bare (conductive), accessible parts of the installation like class I equipment.

As mentioned at the beginning of this contribution, ordinary persons have only had access to operating equipment in the 100 kW range in exceptional cases or not at all. This changed abruptly due to the popularisation of individual electromobility. There is no typical location for electric vehicle charging stations; they can be part of a building installation, in specially constructed charging parks or outdoors at all weather conditions. Depending on the installation site, the design of the protective measures must be considered individually. If the boundary conditions are carefully considered, the protective measure of automatic disconnection of supply in a TN-S system reduces the risk of electric shock in the event of faults in the a.c. low-voltage supply to a conventional level. To meet that requirement, the existing and expected boundary conditions such as conductor lengths, equipotential bonding, existing other installations and the electromagnetic interference, but also environmental influences must be considered.

Both faulty charging stations are supplied by line-conductors with 95 mm^2 cross-section and a 50 mm^2 protective earthing conductor. According to Table 54.2 in [13], the requirement of the minimum cross-section of the protective earthing conductor must be half of the line-conductor is fulfilled. From the results of both faults it can be derived, a higher protective earthing conductor's cross-section would bring advantages and in order to reduce the active fault voltages at the enclosure of the faulty charging station. This would decrease the body impedances and body currents in any current path when touching the enclosures. For the safe operation the functionality of the protective earthing conductor must be ensured. This can be done by regularly testing for example of the fault impedance.

Also, electrical faults can occur at other installation parts than the charging stations e.g. line-to-earth short-circuits in the supply cables or at the transforming station on the low or high voltage level. Such faults also can cause local or transferred electrical potentials and unwanted vagabonding currents in the entire installation which lead to active fault voltage and body currents. To minimize the risk of a harmful electric shock of humans to a conventional level, the whole system from the high voltage to the low voltage level has to be coordinated.

In any case, improper use is not negligible. To ensure that the charging stations and their belonging equipment are safe and reliable after commissioning, they must be regularly tested for verification by persons with appropriate technical expertise.

5.5 Proposal for technical standardisation work

Standardisation today is still lagging behind nationally and internationally in the area of construction and safe operation of electric vehicle charging stations. In the area of safe and reliable operation, the research project ProSafE^2 (Protection, Safety and Efficiency of Electric Vehicle Charging Stations, [15]) is investigating the topic of periodic testing of d.c. charging stations. The results are regularly presented to the Austrian OVE working group AG Ladestationen—DC and, if accepted, also implemented in the OVE directive R 30 [16]. This approach of ProSafE^2, with the OVE as project leader, whose working group is made up of research institutes, industry, grid operators and energy supply companies, a testing and certification institute as well as operators of charging stations, is exemplary and can only be supported and increased in other standardisation projects. However, the manufacturers of charging stations should also become increasingly involved here in order to coordinate the protective measures from the power supply to the load in the best possible way.

Acknowledgements The ProSafE^2 project is funded in the Collective Research Call (part of 'Basisprogramm') of the Aus-

trian Research Promotion Agency (FFG) and supported by the industry partners Energie Steiermark, KELAG, Wien Energie and TÜV Austria.

Funding Open access funding provided by Graz University of Technology.

References

1. Ruehli AE, Antonini G, Jiang L (2017) Circuit oriented electromagnetic modelling using the peec techniques. The Institute of Electrical and Electronics Engineers, IEEE press. John Wiley & Sons, Hoboken
2. IEC 60479-1 Edition 1.0: 2018-12, Effects of current on human beings and livestock—Part 1: General aspects
3. IEC 60479-2 Edition 1.0: 2019-05, Effects of current on human beings and livestock—Part 2: Special Aspects
4. IEC 60479-3: 1998-09, Effects of current on human beings and livestock—Part 3: Effects of currents passing through the body of livestock
5. IEC/TR 60479-4 Edition 2.0: 2011-10, Effects of current on human beings and livestock—Part 4: Effects of lightning strokes
6. IEC/TR 60479-5 Edition 1.0: 2007-11, Effects of current on human beings and livestock—Part 5: Touch voltage threshold values for physiological effects
7. IEC/TR 60479-5 Edition 1.0: 2007-11, Effects of current on human beings and livestock—Part 5: Touch voltage threshold values for physiological effects, Corrigendum 1, 2013–08
8. Bachl H, Biegelmeier G, Hirtler R (2001) Körperimpedanzen des Menschen bei trokkenen, wassernassen und salznassen Berührungsflächen verschiedener Größe. ESF-Bericht, vol 2. Gemeinnützige Privatstiftung Elektroschutz
9. Antoni H, Biegelmeier G, Kieback D (2001) Konventionelle Grenzwerte mit vertretbarem Risiko für das Auftreten von Herzkammerflimmern bei elektrischen Durchströmungen mit Wechselstrom 50/60 Hz bzw. Gleichstrom. ESF-Bericht, vol 3. Gemeinnützige Privatstiftung Elektroschutz
10. Biegelmeier G (2001) Schutz gegen elektrischen Schlag, Beurteilung der Grenzrisiken, Wertigkeitsvergleiche. ESF-Schriftenreihe, vol 4. Gemeinnützige Privatstiftung Elektroschutz
11. Fürnschuß M, Pack S, Schmautzer E, Hofbauer F, Kowatsch G, Dörfler J, Schürhuber R (2023) Investigations of electrical interference of vertical earth rod arrangements. e&i Elektrotech Inftech. https://doi.org/10.1007/s00502-023-01121-9
12. Fürnschuß M, Pack S, Schmautzer E, Schürhuber R (2023) Investigations of 3D meshed earthing systems. In: 27th International Conference on Electricity Distribution, Rome 06-2023
13. OVE E 8101:2019-01-01 + AC1:2020-05-01, Elektrische Niederspannungsanlagen
14. Koch W (1961) Erdungen in Wechselstromanlagen über 1 kV, 3rd edn. Springer, Berlin, Göttingen, Heidelberg
15. OVE Österreichischer Verband für Elektrotechnik Forschungsprojekt ProSafE2. https://www.ove.at/energiewende/projekt-prosafe2/. Accessed 9 Aug 2023
16. OVE-Richtlinie R 30: 2020-08-01, Sicherer Betrieb von elektrischen, konduktiven Ladeeinrichtungen für Elektrofahrzeuge mit einer Nennspannung bis AC 1000 V und DC 1500 V

Further References

17. Herbst D, Schaupp C, Fürnschuß M, Reichel P, Lehfuß F, Stainer T (2023) Projekt ProSafE2 Erstes Forschungsjahr erfolgreich abgeschlossen. e&i Elektrotechnik und Informationstechnik 2023(3-4):a27–a30
18. Herbst D, Fürnschuß M, Schürhuber R, Reichel P, Lehfuss F, Auer C, Schmautzer E (2023) DC Electric vehicle charging infrastructure—Methods for periodic verification. In: 27th International Conference on Electricity Distribution, Rome 06–2023
19. Herbst D, Fürnschuß M, Reichel P, Lehfuss F, Auer C, Schmautzer E (2022) Challenges and related solutions for periodic verification of DC electric vehicle charging stations. In: CIRED workshop on E-mobility and power distribution systems, Porto 06-2022
20. Wenner F (1915) A method of measuring earth resistivity. Bulletin of the Bureau of Standards 12:469–478
21. DKE-IEV Deutsche Online-Ausgabe des International Electrotechnical Vocabulary, DKE Deutsche Kommission Elektrotechnik Elektronik Informationstechnik in DIN und VDE. https://www2.dke.de/de/online-service/dke-iev/Seiten/IEV-Woerterbuch.aspx. Accessed 27 July 2023

Martin Fürnschuß, is a PhD student at the Institute for Electrical Power Systems at Graz University of Technology. Main research interests: Earthing, Transients, EMI, EMC, EMF, protection against electric shock, safety of DC-EVCSs, photovoltaics.

Daniel Herbst, is a PhD student at the Institute for Electrical Power Systems at Graz University of Technology. Within the scope of his current activities he is working on the topics of protection concepts in the area of low voltage, protection against electric shock (protective measures), standardization, safety of DC electric vehicle charging stations and measurement technology in electrical power systems.

Peter Reichel, studied Technical Physics at the Vienna University of Technology. Also, he studied International Innovation and Technology Management at the Linzer Management Academy—LIMAK and the Johannes Kepler University Linz. Among other duties, he has been serving as Secretary General of the Austrian Electrotechnical Association and Chief editor of the journal e+i since 2004.

Daniel Stahleder, currently holds the position of Research Engineer at the Business Unit for Electric Energy Systems at the Austrian Institute of Technology. His primary area of expertise lies in e-mobility charging infrastructure, with a specific focus on grid integration, conformance testing, and charging communication.

Christian Auer, is project engineer at Kristl, Seibt & Co GmbH (KS Engineers). His main professional interests are EMC and power electronics.

Ernst Schmautzer, was a Senior Scientist at the Institute of Electrical Power Systems at Graz University of Technology and is now active as a consultant after his retirement. Professional activities: Inductive, ohmic and capacitive interference, ac-corrosion, grounding and equipotential bonding systems, protection measures, low-voltage electrical installations, low-frequency electromagnetic fields, efficient use of electrical energy, load management, smart buildings, smart grids.

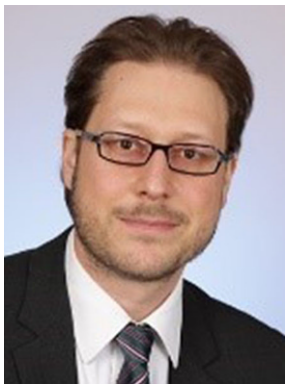

Robert Schürhuber, received his PhD in electrical engineering from the Vienna University of Technology in 2003. From 2003 to 2017, he worked in various areas of electrical power engineering for the companies Siemens and Andritz Hydro, and was also a lecturer in the field of electrical power engineering at the Vienna University of Technology. Since October 2017, he has headed the Institute for Electrical Systems and Networks at Graz University of Technology.